in Fig. 3. Figure 3 shows the separate partial-wave contributions to the $2\,^3S$ cross section, their sum, and the experimentally obtained integrated $2\,^3S$ excitation cross sections of Ref. 1. The structure in the total cross section at 50 eV is seen to be due to the $P$-wave contribution to the cross section in agreement with the measurements of Ref. 1, while an additional $P$-wave structure at about 60 eV is also seen. The effect of other resonances in other channels will be discussed in a subsequent publication.

[1a]G. B. Crooks, R. D. Dubois, D. E. Golden, and M. E. Rudd, Phys. Rev. Lett. 29, 327 (1972).
[1b]G. B. Crooks, Ph.D. thesis, University of Nebraska, 1972 (unpublished).
[2]S. Trajmar, Phys. Rev. A 8, 191 (1973).
[3]R. I. Hall, G. Joyez, J. Mazeau, J. Reinhardt, and G. Schermann, to be published.
[4]R. W. La Bahn and J. Callaway, Phys. Rev. 147, 28 (1966), and Phys. Rev. A 2, 366 (1970).
[5]I. Eliezer and Y. K. Pan, Theor. Chim. Acta 16, 63 (1970).
[6]C. A. Nicolaides, Phys. Rev. A 6, 2078 (1972).
[7]K. Smith, D. E. Golden, S. Ormonde, B. W. Torres, and A. R. Davies, Phys. Rev. A (to be published).
[8]J. A. Slevin, P. J. Visconti, and K. Rubin, Phys. Rev. A 5, 2065 (1972).
[9]D. G. Truhlar, S. Trajmar, W. Williams, S. Ormonde, and B. Torres, Phys. Rev. A (to be published).
[10]P. G. Burke, J. W. Cooper, and S. Ormonde, Phys. Rev. 183, 245 (1969).
[11]J. Macek, Phys. Rev. A 2, 1101 (1970).
[12]A detailed description of the calculations and other results obtained are in preparation for publication under separate cover.
[13]H. S. Taylor, G. V. Nazaroff, and A. Golebiewski, J. Chem. Phys. 45, 2872 (1966).
[14]A. L. Sinfailam and R. K. Nesbet, Phys. Rev. A 6, 2118 (1972).
[15]D. E. Golden, F. D. Schowengerdt, and J. Macek (to be published).

# Interatomic Auger Processes: Effects on Lifetimes of Core Hole States

P. H. Citrin
*Bell Laboratories, Murray Hill, New Jersey 07974*
(Received 11 September 1973)

The lifetimes of core hole states, as determined from x-ray photoemission measurements in a variety of materials, is shown to depend on, and in many cases be primarily determined by, an interatomic Auger mechanism involving transitions from ligand valence electrons. Interpretations of linewidths and other spectral features observed from those spectroscopies involving core holes must be re-evaluated in light of these processes.

Recently, it has been shown that the lifetime of core holes in solids[1] and gases,[2] which decay primarily from nonradiative Auger transitions involving the valence electrons *on* the hole-state atom, depend on the chemical nature of that atom. This effect was observed in x-ray photoemission measurements of a series of compounds in which the core hole in the more oxidized species has not only a higher binding energy but also a narrower linewidth as a result of the decreased number of valence electrons available for filling that hole.[1,2] The simple correlation of binding energy with linewidth is, in some cases, obeyed but there are a number of notable cases (discussed below) in which it is not. In this Letter, we present photoemission data which show that in addition to the above-mentioned *intra*-atomic considerations, an *inter*atomic and usually dominating process must also be taken into account.

Consider the matrix element describing an Auger transition. Ignoring exchange, this may be expressed as

$$\langle \varphi_A(1)\Psi(2)|\,|\vec{r}_1-\vec{r}_2|^{-1}|\Phi_{A,B}(1)\Phi'_{A,B}(2)\rangle, \qquad (1)$$

where $\varphi_A(1)$ is the initial hole state on site $A$, $\Psi(2)$ is the continuum state of the Auger electron, and $\Phi(1)$ and $\Phi'(2)$ are the initial bound states of the hole-filling and ejected electrons, respectively. We now make the important distinction that these bound-state wave functions may be localized either on site $A$ (the hole-state atom), site $B$ (the nearest-neighbor ligand to the hole-state atom), or combinations of these two sites. Consistent with this picture, we distinguish among the various possible Auger mechanisms by the notation $AA$, $BB$, $AB$, or $BA$, where the first letter refers to the site from which the hole-filling electron originates and

the second letter refers to the Auger electron site. The relative importance of these mechanisms in a particular system clearly depends on the spatial overlap of state $\varphi_A(1)$ with $\Phi_{A,B}(1)$ and $\Psi(2)$ with $\Phi'_{A,B}(2)$. With this basic consideration in mind, we present experimental evidence for each of these mechanisms and propose methods for determining their relative importance.

The *AA* Auger mechanism is straightforward since only intra-atomic electrons are involved. Examples of this process are seen in monatomic gases and pure metals. By simply increasing the number of electrons available for either hole filling or ejection in these systems, e.g., Ar versus Ne, the lifetimes of the corresponding core hole states decrease.[3]

The *BB* Auger process presents itself in those systems in which higher-lying (lesser-bound) electrons on the hole-state atom are unavailable for hole filling. A typical example of this is seen for the Na $2p$ core hole in NaOH. In contrast to the case of Na metal in which a $2p$ hole decays by simultaneous filling from and ejection of Na $3s$ conduction electrons, this *AA* mechanism is no longer possible here because of the effective removal (ionization) of the Na $3s$ electrons by the hydroxyl ligands. Thus, on the basis of these intra-atomic considerations, one would expect the Na $2p$ linewidth in the hydroxide to be considerably narrow. In point of fact, the linewidths of these electrons measured from x-ray photoemission spectra show that after subtraction of instrumental resolution the Na $2p$ levels in NaOH are more than 5 times broader than in Na.[4] To our knowledge, this in one of the largest chemical effects on lifetimes ever observed (larger effects are given below). We attribute this lifetime broadening to the greater number of hydroxyl valence electrons available for filling both the Na $2p$ photohole and the continuum state.[5] In order for the implications of this effect to be explored more fully for the general case, it is worthwhile at this point to consider the factors governing the probability of such interatomic Auger processes.

The magnitude of the interatomic transition rate, proportional to the square of the matrix element (1) above, depends on the spatial distribution or density of those ligand electrons that are available for hole filling or ejection by virtue of either their overlap with or their proximity to the photohole. The effective density of such electrons will equal the number of them per ligand, $n_L$, times the coordination number of the hole-state atom, $n_C$, all taken over a volume appropriate to that hole-state atom. We now take the very simplified point of view that atoms or ions in a molecule or crystal may be represented as ionic spheres whose "effective" radii, when summed, equal their interatomic or interionic distance $R$. With this assumption, we define the available (ligand) valence electron density (AVED) $D_{VE}$ by the expression

$$D_{VE} = n_C d_L (V_L/V_R) V_{R'}/V_R. \quad (2)$$

Here $d_L$ is the individual ligand valence electron density, equal to $n_L/v_L$, where $v_L$ is the ligand volume. In the next term, $V_L$ is the amount of ligand volume subtended by a sphere of radius $R$, and can be shown to be equal, in units of $v_L$, to $\frac{1}{2}(1 - \frac{3}{8}L/R)$, where $R = L + C$, and $L$ and $C$ are the "effective" radii of the ligand and hole-states species, respectively. Inspection of this second term shows how the spatial fraction of charge density from each ligand is apportioned to the hole-state atom. In order to compare different crystals of different $n_C$ and $R$, the third term in Eq. (2) normalizes the effective density, incorporated in the first two terms, to the case of closest packing of ligands consistent with the molecular or crystal geometry. The various terms appearing in Eq. (2) are illustrated in Fig. 1 for a square planar configuration.

The validity of this approach was tested for the oxides, fluorides, and chlorides of Na,[6] Mg, and Al, in which the concept of ionic spheres is most reasonable. By measuring the x-ray photoemission $2p$ core lines in a given metal for different ligands, the *BB* mechanism is systematically isolated. The data reported here were taken with a Hewlett-Packard 5950A spectrometer for electron spectroscopy for chemical analysis. All samples were in the form of thin

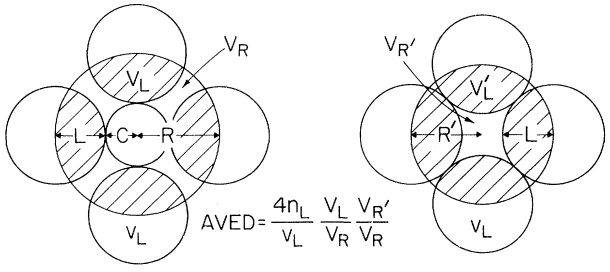


FIG. 1. Determination of available (ligand) valence electron density AVED for a hole-state atom surrounded by four nearest-neighbor ligands in a square planar configuration.

films to reduce charging and were prepared either by evaporation in the spectrometer sample chamber or by chemical growth on metal substrates in an oven. Inhomogeneous charging, checked by methods similar to those elaborated in Ref. 4 for NaOH, was determined to be of very minor significance in these samples. Oxygen and carbon contamination, deduced from *in situ* monitoring of contaminant core lines, was also negligibly small. To test for possible lattice distortion effects on linewidths, measurements on thin films and single crystals of NaF and $MgF_2$ were performed; the results for both cases were virtually identical. Linewidths were determined by a nonlinear least-squares fitting procedure with line shapes adjustable between Gaussian and Lorentzian. The appropriate atomic $2p$ spin-orbit splittings[7] and the relative intensities of the spin-orbit components were fixed input parameters. The shapes of the measured lines (including the spectrometer function) were determined from the fit to be essentially Lorentzian, as expected from lifetime considerations. For simplicity, the effective instrumental resolution of $0.53 \pm 0.06$ eV, determined from the shape of metal Fermi edges, was assumed to be Lorentzian. A typical spectrum of Al $2p$ electrons in $AlF_3$ grown on Al metal, along with the computer fits superposed on the raw data, is shown in the inset in Fig. 2.

The AVED's were calculated from Eq. (2) assuming the six valence $p$ electrons of the fluoride, chloride, and oxide ligands to be most available for ejection or photohole filling as a result of their relatively large radial extent. Values of "effective" radii were taken from a recent compilation by Shannon and Prewitt.[8]

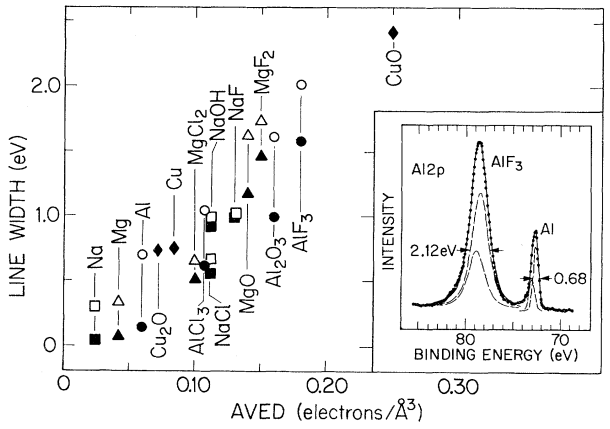


FIG. 2. AVED versus linewidth of core electrons in a variety of compounds. Filled symbols, $2p_{3/2}$ linewidths; open shapes, $2s$ linewidths. The linewidths plotted do not include instrumental resolution. Inset, Al $2p$ electrons from a thin film of $AlF_3$ on an Al substrate. Linewidths at full width at half-maximum of the least-squares–fit spin-orbit components (only $2p_{3/2}$ shown above) include instrumental resolution.

The metal $2p_{3/2}$ linewidths (filled shapes) versus AVED are plotted and shown in Fig. 2. For purposes of clarity, possible systematic errors arising from instrumental line shape and linewidth assumptions have not been indicated; errors from the fitting procedure are typically $< 0.05$ eV. It is interesting to note that while the linewidths are predicted to depend on the appropriate AVED's for compounds of a particular metal, empirically it is found that by dividing the AVED's for Mg and Al compounds by factors of 2 and 3, respectively, an approximately linear relationship of uniform slope for all compounds is obtained. The important point to be made here, however, is that, regardless of slope factors, a definite correlation of linewidth (lifetime) with AVED is observed for all these materials—in marked contrast to the trend in the opposite direction predicted on the basis of intra-atomic effects. This correlation, then, provides firm evidence for the importance of the interatomic mechanism.

Having established this result, we are now in a position to compare and understand the relationship of the *BB* with the *AA* and *AB* mechanisms. For the case of the *AA* process, the narrow linewidths observed in free-electron-like metals, for example, may be understood as follows. Since the ion core in such a metal is essentially the same as that of its ionized species, the AVED of that metal may be taken as simply equal to the number of valence electrons per metal atom divided by the volume of that atom in the metal. The AVED's of Na, Mg, and Al calculated in this way are shown in Fig. 2, with the Mg and Al AVED's divided by 2 and 3 as above. We see from this figure that the basic physical phenomenon of fewer available electrons in the metal relative to its oxidized species, as reflected in the appreciably smaller metal AVED's, is clearly demonstrated.[9]

The *AB* mechanism presents perhaps the most interesting case since either the intra-atomic (*A*) or interatomic (*B*) effects may be varied.[10] We may easily do the latter through measurements of the metal $2s$ holes in the Na, Mg, and Al compounds studied above. In this way, the very efficient Coster-Kronig (intra-atomic)

mechanism is kept essentially constant in a given metal series, while the nature of the ligands is systematically varied. A plot of the 2*s* linewidths (shown as open shapes) versus AVED is presented in Fig. 2 from which the correlation with the environment is again apparent.

A dramatic example of the predominance of the interatomic effect in the *AB* mechanism is seen in the series Cu, $Cu_2O$, and CuO. Analogous to the metals considered above, we take the Cu $3s^23p^63d^{10}$ electrons in Cu and $Cu_2O$ as the core in which intra-atomic processes are essentially the same and assume likewise for the Cu $3d^9$ configuration in CuO.[11] The Cu 2*p* linewidths in these materials have been included in Fig. 2. Considering that these electrons are bound by more than 900 eV, that their lifetimes are in part influenced by strictly intra-atomic processes (e.g., *LMM*), and that the trend of their linewidths with formal charge state is nonmonotonic, the agreement with the calculated AVED is most gratifying. (The Cu $2p_{3/2}$ width in $Cu_2O$ is so narrow because of its unusually low $n_C$ of 2.)

An example of an *AB* mechanism in which the intra-atomic processes predominate is seen in the series $V_2O_3$, $VO_2$, and $V_2O_5$. Here, the core electron configuration changes appreciably from V $3s^23p^63d^2$ in $V_2O_3$ to V $3s^23p^6$ in $V_2O_5$, while variations in the calculated AVED's change no more than 20%. The measured linewidths[12] in these compounds follow the intra-atomic trend and are correlated with the V 2*p* binding energies, as predicted.[1,2]

It is worth noting here that although the majority of examples sited above are given in solids, these effects clearly present themselves in gases. Thus, effects otherwise anomalous by intra-atomic considerations, e.g., the C 1*s* linewidths in carbon suboxide[1,2] and those of F 1*s* in $CF_4$ and $CH_3F$,[13] may be easily understood in terms of the dominating effects of the interatomic processes.

Finally, we mention some general conclusions and implications of the above study: (1) The lifetimes of core hole states depend on both intra-atomic and interatomic electron contributions, with the latter effects sometimes completely dominating. (2) Linewidths and other spectral features observed in not only x-ray photoemission, but also in x-ray absorption and emission and Auger[14] spectroscopies, must be interpreted in terms consistent with these interatomic processes. (3) As a consequence of these processes, there is an inherent, sometimes severe limitation on the effective resolution obtainable in all of these techniques.

The author thanks P. M. Eisenberger and D. R. Hamann for helpful comments and suggestions, and H. J. Guggenheim for preparation of the oven-grown samples.

[1]R. M. Friedman, J. Hudis, and M. L. Perlman, Phys. Rev. Lett. 29, 692 (1972).

[2]R. W. Shaw, Jr., and T. D. Thomas, Phys. Rev. Lett. 29, 689 (1972).

[3]See, for example, K. Siegbahn *et al.*, *ESCA Applied to Free Molecules* (North-Holland, Amsterdam, 1969), p. 24.

[4]P. H. Citrin, Phys. Rev. B (to be published).

[5]Possible spurious core line broadening from inhomogeneous sample charging has been ruled out in Ref. 4 by a variety of methods, while possible broadening from crystal field or banding effects is insignificant for core levels such as Na 2*p*.

[6]Pure $Na_2O$ could not be measured as a result of NaOH contamination, so results for NaOH (Ref. 4) were used instead.

[7]C. E. Moore, *Atomic Energy Levels as Derived from Analyses of Optical Spectra*, National Bureau of Standards Circular No. 467 (U. S. GPO, Washington, D. C., 1949).

[8]R. D. Shannon and C. T. Prewitt, Acta Crystallogr., Sect. B 25, 925 (1969).

[9]Although the spatial distributions of the metal valence (conduction) electrons are quite different from those of the ligand *p* wave functions, the small metal AVED values do not significantly reflect this difference.

[10]From overlap considerations, the *BA* mechanism is an unlikely one.

[11]These assumptions are justified from our photoemission measurements of (1) similar valence band spectra in Cu, $Cu_2O$, and CuO, and (2) negligibly small multiplet splittings observed for Cu 2*s* electrons in CuO.

[12]G. K. Wertheim, to be published.

[13]T. D. Thomas, J. Amer. Chem. Soc. 92, 4184 (1970).

[14]P. H. Citrin, to be published.